International Conference on Space Optics—ICSO 2018

Chania, Greece

9–12 October 2018

Edited by Zoran Sodnik, Nikos Karafolas, and Bruno Cugny

ATHENA Telescope: alignment and integration of SPO mirror modules

G. Valsecchi

F. Marioni

G. Bianucci

F. Zocchi

et al.

International Conference on Space Optics — ICSO 2018, edited by Zoran Sodnik, Nikos Karafolas, Bruno Cugny, Proc. of SPIE Vol. 11180, 111801N · © 2018 ESA and CNES · CCC code: 0277-786X/18/$18 · doi: 10.1117/12.2535978

ATHENA Telescope: alignment and integration of SPO mirror modules

G. Valsecchi*[a], F. Marioni[a], G. Bianucci[a], F.E. Zocchi[a], D. Gallieni[b], G. Parodi[c], M. Ottolini[c], M. Collon[d], G. Pareschi[e], D. Spiga[eh], M. Bavdaz[f], E. Wille[f], V. Burwitz[g], G. Hartner[g], C. Pelliciari[g]
[a]Media Lario S.r.l., Località Pascolo, 23842 Bosisio Parini, Italy
[b]A.D.S. International S.r.l., via Pio Galli sind. 3, 23841 Annone B.za, Italy
[c]BCV Progetti S.r.l., Via S. Orsola1, 20123 Milano, Italy
[d]Cosine Research B.V, Oosteinde 36, NL-2361 HE Warmond, The Netherlands
[e]INAF Osservatorio Astronomico di Brera, Via E. Bianchi 46, 23807 Merate, Italy
[f]European Space Agency, ESTEC, Keplerlaan 1, NL-2200 AG Noordwijk, The Netherlands
[g]MPI für extraterrestrische Physik, 85748 Garching, Munich, Germany
[h]SLAC National Accelerator Laboratory, 2575 Sand Hill Road, Menlo Park CA 94025

ABSTRACT

ATHENA (Advanced Telescope for High-ENergy Astrophysics) is the next high-energy astrophysical mission of the European Space Agency currently planned to be launched in the early 2030s, as part of its Cosmic Vision program, on the scientific topic of "Hot and Energetic Universe". The optics technology is based on the Silicon Pore Optics (SPO). About 678 SPO mirror modules will have to be integrated and co-aligned onto the optical bench of the Mirror Assembly Module (MAM) of ATHENA. This activity will have to be completed in about two years. Media Lario leads an industrial and scientific team that has developed the process to align and integrate the SPO Mirror module with an accuracy better than 1 arcsec. The process is based on position of the centroid of the point spread function produced by each mirror module when illuminated by a collimated planewave at 218 nm taken at 12 m focal length. Experimental tests, using two SPO mirror modules, and correlation with X-ray measurement at the PANTER test facility in Münich have demonstrated that this process meets the accuracy requirement. It was also demonstrated, that a mirror module can be removed again from the MAM, and re-installed, without compromising the adjacent mirror modules. This technique allows arbitrary integration sequence and integration of two Mirror Modules per day. Moreover, it enables monitoring the telescope point spread function during the whole integration phase.

Keywords: X-ray optics, X-ray telescopes, ATHENA, Silicon Pore Optics, Integration, Optical Alignment.

1. INTRODUCTION

The ATHENA (Advanced Telescope for High-ENergy Astrophysics) mission [1]-[3] of the European Space Agency is based on an X-ray telescope with a focal length of 12 m and an angular resolution of 5 arcsec half energy width (HEW). The telescope consists in a 2.5 m circular supporting structure on which about 678 SPO Mirror Modules (MM) [4][6] are aligned and integrated on a vertical optical bench that is used to capture the focal plane image of each SPO MM while illuminated by a planewave having a wavelength of 218 nm. The light emitted by the UV source is reflected by a parabolic collimator mirror to generate a beam, thus simulating illumination from a point-like deep space source. The MM focuses the collimated beam onto a CCD camera placed at the 12 m focal position and the acquired point spread function (PSF) is processed in real time to calculate the centroid position and intensity parameters. This information is then used to guide the robot-assisted alignment sequence.
This alignment and integration process has been successfully adopted in the past by Media Lario for the integration of the Mirror Modules of many X-Ray Telescopes, such as Beppo-SAX, JET-X, SWIFT, XMM-Newton and eROSITA [8].

Media Lario together with A.D.S. International, BCV Progetti, Cosine, INAF-OAB, and TAS-I have demonstrated that this alignment and assembly process is also working for the integration of the SPO MMs into the ATHENA telescope.

giuseppe.valsecchi@medialario.com; phone +39 031 867111; medialario.com

The process has the following distinguishing characteristics:

- alignment accuracy within the 1 arcsec goal (error budget allocated for integration).
- implementation in standard ISO 5/6 cleanroom (no vacuum infrastructure needed);
- integration of 2 MMs per day, equivalent to 2-year total integration time for the entire telescope;
- arbitrary integration sequence of the 678 MMs;
- option to remove, re-align, or replace any MM in any integration sequence scenario;
- full-telescope illumination, to monitor the optical performance during integration;
- easy telescope dismount/realign procedures for intermediate tests at X-ray facilities.

In this paper, the detailed integration process and the results on the demonstrator having 2 MMs, are reported.

2. ALIGNMENT ERROR BUDGET

The main driver for the definition of the alignment metrology and procedure and for the design of the telescope structure is the error budget for the angular resolution of the ATHENA telescope, as set by the Agency (Table 1).

The integration of 678 MMs has a total allocated error budget of 1.5 arcsec (goal 1 arcsec). We have further broken this global error value into specifications for a single MM, which has then become the main performance driver for the metrology and integration process. We have assumed the following simplified one-dimensional model:

1. all MMs have the same PSF on the telescope focal plane;
2. the PSF of each MM is described by a one-dimensional Gaussian function;
3. the effective area is the same for all MMs;
4. the distribution of the alignment error is a one-dimensional Gaussian function.

The effect of the MMs alignment errors is simulated by the centroid shift of each MM, described with a one-dimensional Gaussian distribution with standard deviation σ. The total PSF is the convolution of the PSF of the MMs with their centroid shifts, both described by one-dimensional Gaussian distributions. The convolution is also a Gaussian function with variance equal to the sum of the variances of the two original Gaussian functions. Therefore, the HEW of the entire telescope is given by

$$\mathrm{HEW}_{\mathrm{Population}} = \sqrt{\mathrm{HEW}_{\mathrm{MM}}^2 + (1.349\sigma_{\mathrm{centroids}})^2}$$

where 1.349 is the ratio between the HEW and the standard deviation for a one-dimensional Gaussian function. Since the goal for the HEW of each MM is 2.5 arcsec and 1 arcsec is allocated in quadrature for the MMs alignment and integration error, the HEW of the entire integrated MM population is 2.7 arcsec. Consequently, the σ of the distribution of the centroids after integration must be smaller than

$$\sigma_{\mathrm{centroids}} \leq \frac{1}{1.349}\sqrt{\mathrm{HEW}_{\mathrm{Population}}^2 - \mathrm{HEW}_{\mathrm{MM}}^2} = \frac{1}{1.349} = 0.74 \text{ arcsec}$$

Therefore, 0.74 arcsec is the error budget (standard deviation) allocated for the alignment of each individual MM in order to meet the 1 arcsec error budget goal for the entire population of 678 MMs.

Table 1. HEW error budget for the ATHENA telescope.

HEW telescope error budget	**Requirement [arcsec]**	**Goal [arcsec]**
Mirror Module	4.3	2.5
Alignment and integration	1.5	1.0
Distortions	1.5	1.0
Spacecraft related	1.0	0.5
Margin	1.0	0.5
Root Square Sum	**5.0**	**3.0**

Table 2. Sub-system integration error budget for the demonstrator and for the FM (X, Y, Z correspond to azimuthal, radial and optical axis coordinates).

Sub System	Parameter	Demonstrator	Flight module
Telescope integration	HEW	< 1.5 arcsec	< 1.5 arcsec
	Effective area loss	< 5%	< 1%
MM accuracy	Accuracy of MM focal length	< 5 mm	< 1.5 ÷ 2.5 mm
	X and Y alignment accuracy of brackets	< 0.5 mm	< 0.5 mm
MM alignment	Maximum X and Y errors	< 12 µm	< 12 µm
	Maximum R_X error	< 100 arcsec	< 10 ÷ 30 arcsec
	Maximum R_Y error	< 400 arcsec	< 30 ÷ 120 arcsec
Optical bench	Collimation of UV illumination beam	> 41 km	> 95 km
	Collimation stability	> 41 km	> 1500 km
	Z position accuracy of the source	< 160 µm	< 380 µm
	Z position stability of the source	< 160 µm	< 23 µm
	Z position accuracy of the CCD camera	< 3.5 mm	< 1.5 mm
	Z position stability of the CCD camera	< 3.5 mm	< 93 µm
	R_Z stability during curing	< 3.2 arcsec	< 1.5 ÷ 9 arcsec

Starting from the high-level telescope requirements, a set of lower level specifications for the main subsystems and components has been derived. They include the alignment tolerance of the mirror modules, the accuracy and stability of the optical bench and the optical performance of the mirror modules. This set of requirements is summarized in Table 2 for both the demonstrator and, preliminarily, the flight module.

3. INTEGRATION FACILITY

The optical bench is schematically shown in Figure 1.

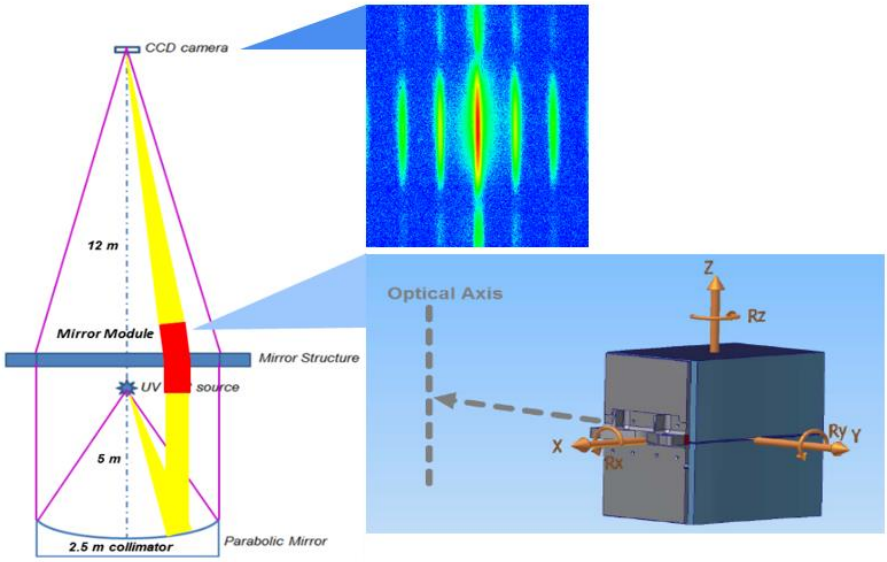

Figure 1. Schematic illustration of the alignment setup and facility.

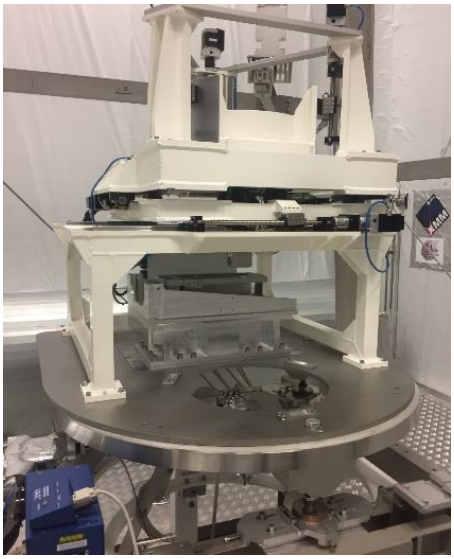

Positioning	Range	Adjustment step
X translation	±100 mm	±0.5 µm
Y translation	–25 ÷ +90 mm	±0.5 µm
Z translation	120 mm	±0.5 µm
X rotation	± 2°	±2 arcsec
Y rotation	± 2°	±2 arcsec
Z rotation	360°	±0.5 arcsec

Figure 2. The robotic handler mounted on the optical bench (left) and positioning range and adjustment steps (right).

The light source is a broadband incoherent lamp from Energetiq Technology Inc., with a diverging beam that illuminates a 780 mm diameter parabolic collimator through a 50 µm pinhole. The light is reflected by the parabolic collimator into a planewave. The incident planewave is then focused by the SPO MM on a CCD at 12 m. The broadband light is filtered at the focal plane by a 20 nm bandpass filter centred at 218 nm. The source power in this bandwidth is of the order of few nanowatt. The CCD camera, from Princeton Instruments, has 1024×1024 square pixels of 13 µm in side. We use a 2×2 pixels binning strategy, resulting in an effective pixel size of 26 µm corresponding to 0.45 arcsec over the 12 m focal length.

The alignment of the MM is performed by a manipulator, the Handling and Alignment Device (HAD), which allows movements in all 6 degrees of freedom around the virtual pivot point defined at the intersection plane between the primary and secondary SPO stacks. The HAD has been designed and realized by the team and all the features of the machine are representative of a full-scale unit. In its full-scale implementation, the robotic handler will provide:

- magnetic pick-and-place of any MM;
- fine positioning (X,Y,Z) and orientation of any MM of any row and azimuth;
- accessibility in the narrow gaps between MMs of different rows;
- Rz, R_X and R_Y (rotation around Z, X and Y axis) fine-alignment capability;
- holding the MM alignment during curing of the bonding material.

The robotic handler is mounted on the optical bench as shown in Figure 2 and provides accurate control of the MM in all its six degrees of freedom, as detailed in the table. The X, Y, Z axis are controlled by seven linear stages with recirculating ball screws driven by stepper motors. The rotation R_Z around the optical axis Z is controlled by a fully-steerable 360° rotator mounted on a custom worm-wheel coupled to a precision and ultra-thin-section bearing. R_X and R_Y are made by linear motors pushing around the pivot points of the two axis.

4. MIRROR STRUCTURE DESIGN

A trade-off of the Mirror Structure to be used for the flight Telescope, including petal and monolithic solutions, with different materials has been performed. Titanium alloy, INVAR 36, and SiC were considered. The structural and thermal analyses were performed for these six cases; finally the monolithic Mirror Structure in Titanium alloy was selected. The monolithic configuration has the following advantages w.r.t the petal configuration:

- Reduced levels of structural components, making the structures more simple
- More efficient structural in terms of stiffness
- Reduced obscuration

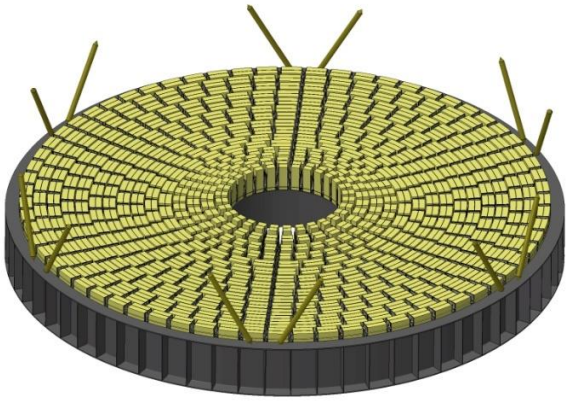

Figure 3. Mirror structure configuration

The walls of the MAM contain the dowel pin housings. The dowel pins act as mechanical interfaces between the MM and the mirror structure. A proper quantity of adhesive is dropped in the housing hole before inserting the DP, then controlling the adhesive overflow.

5. MIRROR MODULE ALIGNMENT AND INTEGRATION

The MM alignment consists of three steps that determine the best orientation of the MM in all its six degrees of freedom illustrated in Figure 1. The alignment is guided by specific parameters calculated from the 218 nm MM focal plane image acquired by the CCD camera [10]:

- maximization of photon count, for rotation R_X and R_Y around X and Y, respectively;
- the position of the image centroid, for rotation R_Z around Z and displacements ΔX and ΔY along X and Y;
- mechanical reference, for displacement ΔZ along the optical axis Z.

The robotic handler is used to move and align the MM over the correct position of the mirror structure. The robotic handler holds the MM with two calibrated flexures that have three small magnets to hold the MM from the Invar brackets (two flanges attached to the MM for handling and integration), as shown in Figure 5.

In more detail, the first step of the process is the alignment of the MM in tip (R_X) and tilt (R_Y) until the intensity of the focal plane image is maximum. A series of images are acquired at different tip/tilt positions of the MM and their intensity values (i.e. photon count) are plotted as function of the tip/tilt values (Figure 6). The best tip/tilt position is at the maximum of each plot, that is the position with minimum vignetting.

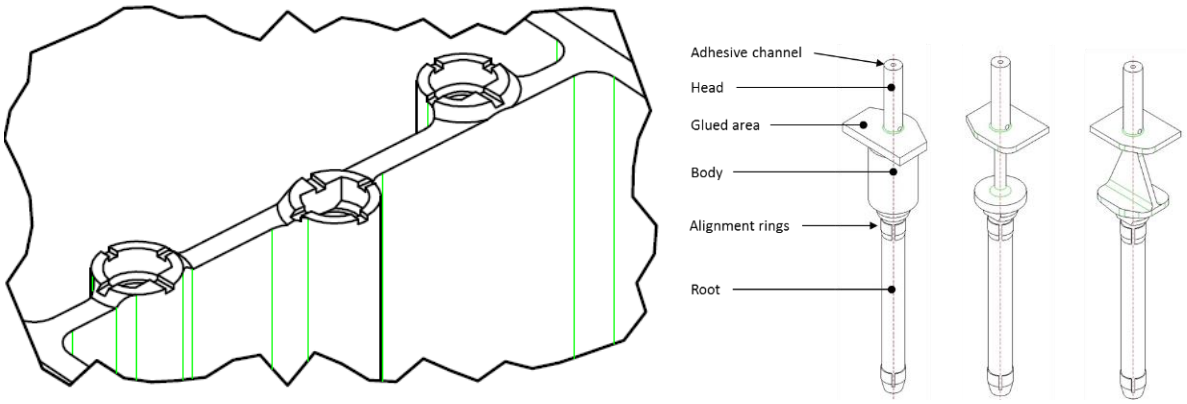

Figure 4. Interface area between the MAM housing (left) and dowel pins (right).

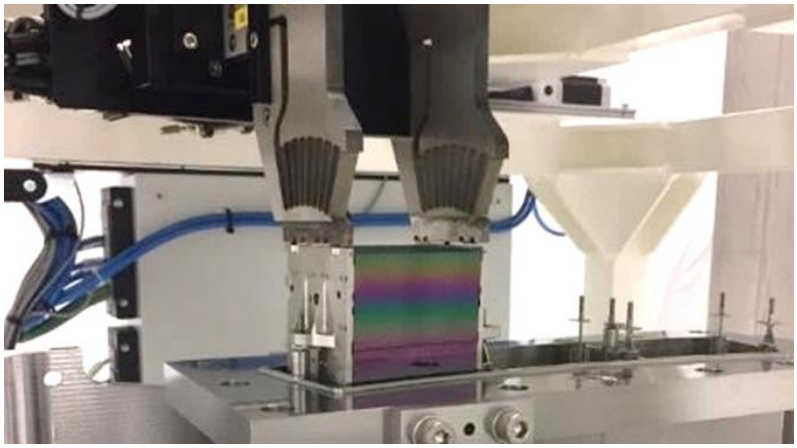

Figure 5. Flexures of the robotic handler holding the MM from the brackets through small magnets.

The second step is the alignment of the MM in rotation (R_Z) and azimuthal position (ΔX), which cause exclusively an X displacement of the centroid. First, the X position of the MM is set so that the dowel pins are approximately centred in the slot holes of the MM bracket. Then the MM is rotated around the Z axis until the centroid is aligned to the X = 0 coordinate of the CCD. This step ends with the alignment of the MM in the azimuthal position ΔY until the centroid of the MM is exactly at the centre of the focal plane, as shown in Figure 7.

The vertical alignment (ΔZ) is adjusted with mechanical reference. First the MM is lowered to touch the dowel pin surface and then it is raised by 100 µm. An electric grounding check between the MM and the mirror structure is used to determine the mechanical contact between the brackets and the dowel pins. This mechanical alignment procedure is accurate enough since the HEW is insensitive to the vertical position of the MM.

After alignment, the MM is finally integrated by adhesive to the mirror structure through the dowel pins, which have previously been bonded to the mirror structure.

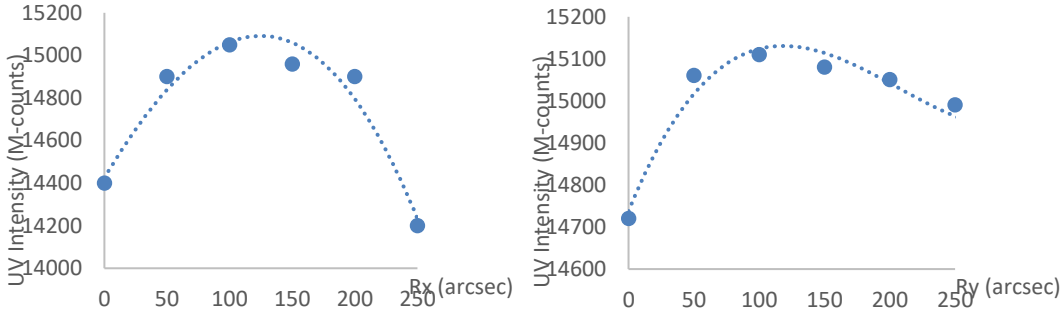

Figure 6. Tip (R_X) and tilt (R_Y) alignment optimization of the MM.

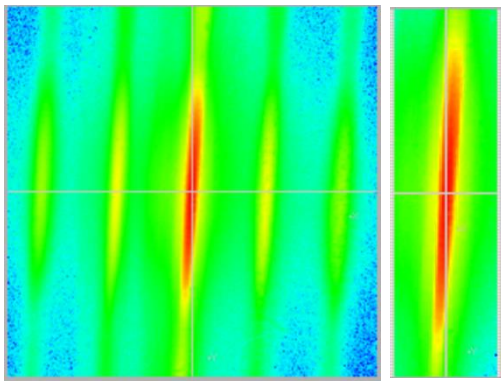

Figure 7. PSF image (left) and area for centroid calculation (right) of aligned MM.

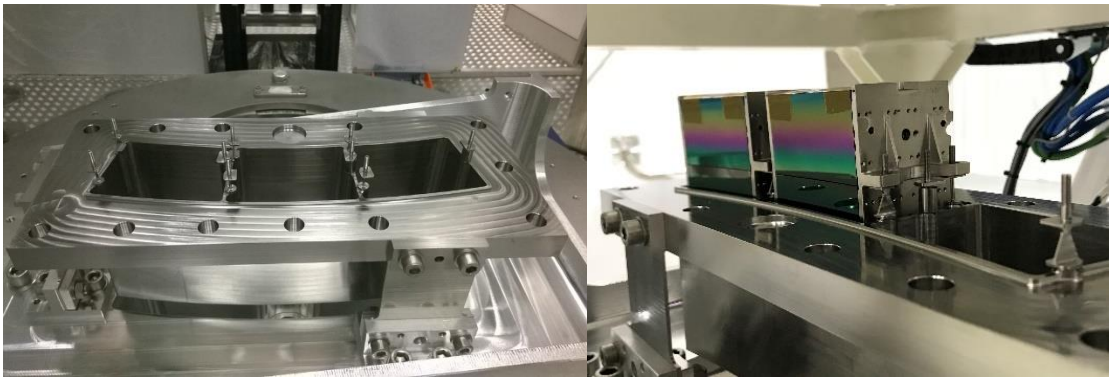

Figure 8. Mirror structure element (left) and Demonstrator with two SPO MMs aligned and integrated.

The dowel pins act as mechanical interfaces between the MM and the mirror structure. After alignment, the MM is in a position in which the top heads of the dowel pins are in the slot holes of the MM brackets. The lateral clearance between the dowel pins and the brackets holes is approximately 0.25 mm, sufficient for the alignment range of the MM. The vertical clearance between the flat shelf of the dowel pins and the corresponding area of the brackets is 0.1-0.2 mm, which is the bonding area for the MM integration. The electric grounding check ensures that there is no mechanical contact between the brackets and the dowel pins.

The top part of the dowel pins has a 0.8 mm channel with two orifices in correspondence of the flat shelf of the pin. While the MM is held in its aligned position by the robotic handler, a controlled amount of epoxy adhesive is injected in the channel to fill, by capillary action, the gap between the bracket and the flat shelf of the pin. The epoxy adhesive has the correct viscosity for an effective capillary flow. Moreover, its low-shrinkage does not impact the alignment during the 16 h, room-temperature curing process, as we have experimentally verified on the optical bench. After curing, the robotic handler is detached from the MM and available for the next MM alignment.

6. INTEGRATION DEMONSTRATOR AND RESULTS

This alignment and integration process has been experimentally verified on a representative ATHENA telescope demonstrator. The demonstrator consists of two SPO MMs integrated in a mirror structure element (MSE) that is an exact cut-out of ATHENA telescope mirror structure (Figure 8). The MSE is made of Titanium and can accommodate up to three MMs spaced by 7.25° in azimuth.

Two MMs were delivered by Cosine [12] and measured at PANTER facility in Munich to verify the performances and the focal length at 1.49 keV before integration. After focus scan, the best x-FWHM was measured for both MMs at 11.963mm. After integration of the MMs into the ATHENA mirror structure element, the demonstrator was delivered again at PANTER to confirm the achieved alignment tolerance. Figure 9 shows the UV and X-ray images of the resulting PSF, with clearly visible overlapped centroids. Figure 10 shows the X-ray x-FWHM and the centroid distance, all plotted against the focal distance [13].

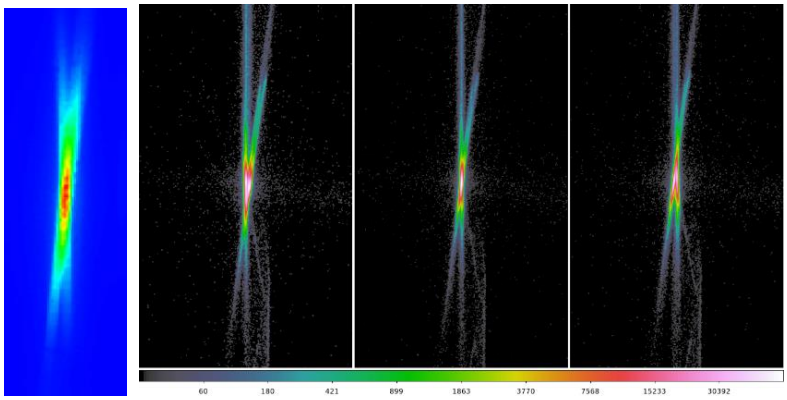

Figure 9. Demonstrator PSF at 218 nm (left) and at 1.49 keV at intra, nominal, and extra focal positions (right).

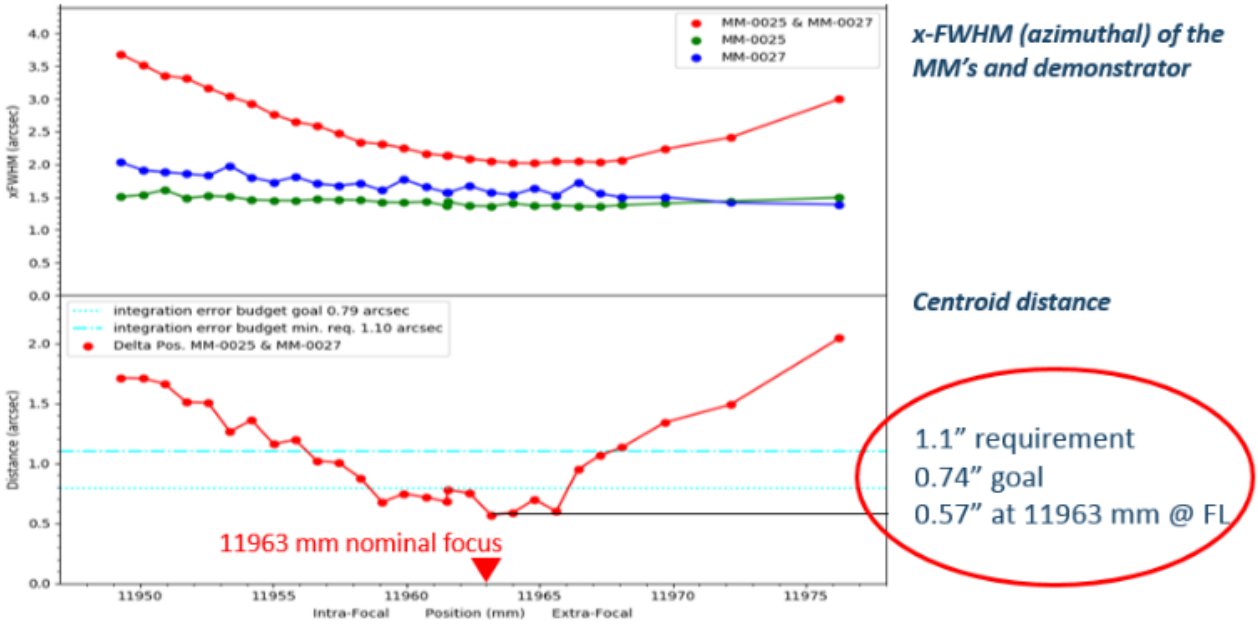

Figure 10. From top to bottom, X-ray HEW, x-FWHM (azimuthal), and distance between the two centroids plotted as a function of the focal distance.

In particular, the bottom graph of Figure 10 showing the difference between the positions of the two MM centroids plotted as a function of the focal distance, confirms that the two MMs have been integrated at their best focal distance of 11,963 mm where the distance between the centroids' positions is the smallest. Consequently, the position difference between the centroids of the 2 MMs corresponds to 0.57 arcsec, well within the allocated budget of 0.74 arcsec discussed in Section 2.

Finally, it should be underlined that MM #0025 has been disassembled from the MSE, cleaned, re-aligned, and bonded again in specification to the same housing of the MSE, as per agreed test plan, without any optical degradation or variation, thus demonstrating the remove-and-replace capability of MMs of the integration process.

7. INTEGRATION FACILITY FOR THE ATHENA TELESCOPE

The conceptual design of the integration facility for the flight phase of the ATHENA project has been assessed and evaluated, including the Ultra-Violet Optical Bench (UVOB) and its building. The UVOB structure is composed by:

- The parabolic collimator mirror,
- UV source support,
- Steel Mirror-Cell containing the parabolic collimator mirror,
- ATHENA Mirror Structure (MS) quasi static support system,
- MM Handling and alignment system with two HADs,
- CCD, UV source, alignment mirrors
- Crane and infrastructure for handling of the ATHENA telescope
- Reinforced concrete foundation block,
- Tower and clean rooms system

The parabolic collimator mirror is the most important component of the facility. The specifications are defined in

Table **3.** The integration facility is built around this mirror and is shown in Figure 11 and Figure 12.

Table 3. Specification of the 2.5 m parabolic collimator of the flight integration optical bench.

Parameter	**Specification**
Function	Collimator mirror in cleanroom laboratory
Shape	Parabolic (concave)
Clear diameter	2,500 mm (tolerance -0/+100 mm TBC)
Focal length	5.1 m (other values acceptable)
External diameter:	Any value that allows full specs in the clear aperture
Central hole:	Not required; if needed for manufacturing, ∅ must be < 400 mm
Material	Zerodur or ULE; CTE up to $3x10^{-6}$ K^{-1} is acceptable
Light-weighting	Not required
Thickness	Sufficient to guarantee optical quality when mounted on supports
Operational position	Face up, optical axis in vertical position, fixed on supports
Mirror cell & supports	Included with the mirror if needed to guarantee optical quality
Operating temp.	20 ± 2 °C
Surface roughness (0.01 – 2 mm)	< 2 nm RMS
WFE slope (range 2 – 20 mm)	± 0.5 arcsec
WFE slope (range 20 – 2,800 mm)	± 0.1 arcsec
Coating reflectivity	>80% in the wavelength range 180 – 240 nm
Coating lifetime	> 4 years in cleanroom

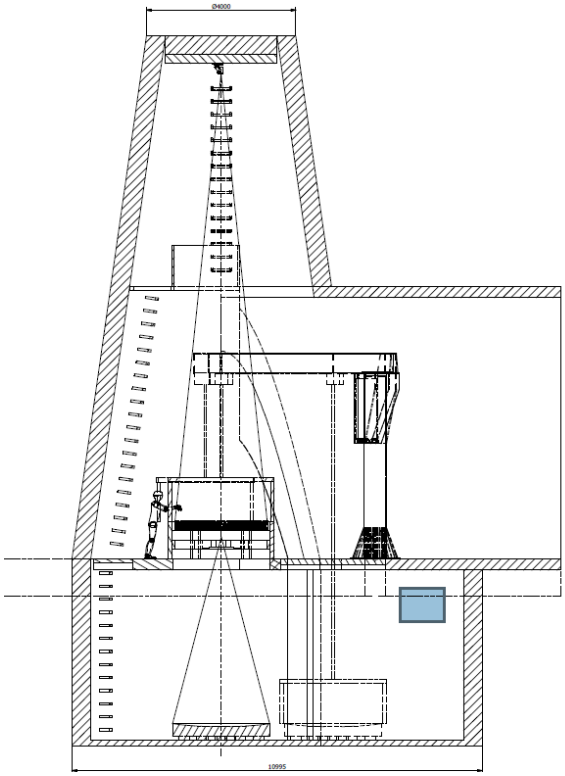

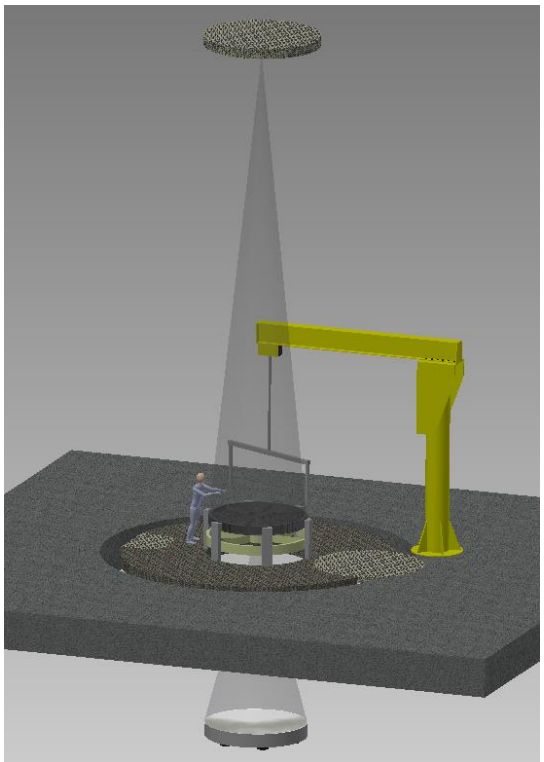

Figure 11. Concept of the UV vertical Optical bench for the ATHENA Telescope integration

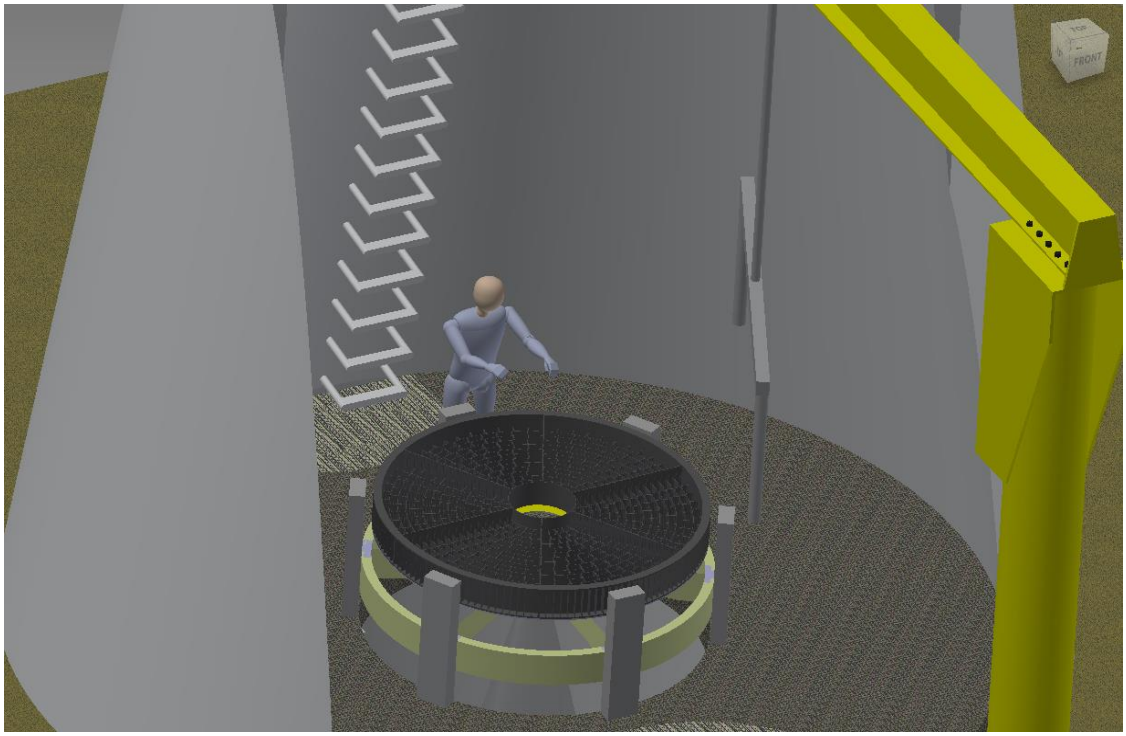

Figure 12. ATHENA telescope during the integration of the SPO mirror module

8. CONCLUSIONS

The process for the alignment and integration of 678 silicon pore optics mirror modules in the 2.5 m diameter structure of the X-ray ATHENA telescope has been developed and tested by Media Lario and the team. The process is based on positioning of the centroid of the point spread function produced by each mirror module when illuminated by a collimated planewave at 218 nm taken with a CCD camera at 12 m focal length.

Demonstration of this process has been successfully carried out at the Media Lario using the UV optical bench with two SPO mirror modules.

The distance between the position of the centroids of the two mirror modules measured at X-ray wavelength at the PANTER test facility resulted to be 0.57 arcsec, well within the 0.74 arcsec goal derived, for each individual MM alignment, from the overall telescope alignment and integration budget of 1 arcsec.

Preliminary design of the UV optical bench needed for the integration of the ATHENA flight telescope has been completed and presented.

ACKNOWLEDGMENT

This work has been done in the framework of the European Space Agency contract 4000114931/15/NL/HB.

REFERENCES

[1] ESA, 2ATHENA: Assessment of an X-Ray telescope for ESA Cosmic Vision Program," CDF-150(A) (2014).
[2] <http://www.the-athena-x-ray-observatory.eu
[3] <http://sci.esa.int/cosmic-vision/54517-athena

[4] Collon, M.J., Vacanti, G., Günther, R., Yanson, A., Barrière, N., et al., "Silicon pore optics development for ATHENA," Proc. SPIE 9603, (2015).
[5] Ayre, M., Bavdaz, M., Ferreira, I., Wille, E., Fransen, S., Stefanescu, A., Linder, M., "ATHENA – System studies and optics accommodation," Proc. SPIE 9905, 990526 (2016).
[6] Bavdaz M.et al."Development of the ATHENA Mirror" Proc. SPIE 10699-32 (2018)
[7] <http://www.mpe.mpg.de/heg/panter>.
[8] Burwitz, V., Predehl, P., Friedrich, P., Bräuninger, H., Eder, J., et. al., "The calibration and testing of eROSITA X-ray mission assemblies," Proc. SPIE 9144, (2014).
[9] Spiga, D., Collon, D.M., Conconi,P., Valsecchi, G., Wille, E., et al., "Optical simulations for design, alignment, and performance prediction of silicon pore optics for the ATHENA X-ray telescope," Proc. SPIE 10399-16 (2017).
[10] Valsecchi G.et al. "Optical integration of SPO mirror modules in the ATHENA telescope," Proc. SPIE 10399-13 (2017).
[11] https://www.helmholtz-berlin.de/quellen/bessy/index_en.html
[12] Collon M. et al., "Silicon Pore Optics Mirror Module Production and Testing," Proc. SPIE 10699-33 (2018)
[13] Valsecchi G. et al., "Results of silicon pore optics mirror modules optical integration of the ATHENA telescope," Proc. SPIE 10699-34 (2018)